# ChemComm



### COMMUNICATION

View Article Online



Cite this: Chem. Commun., 2022, **58**, 997

Received 20th October 2021, Accepted 12th December 2021

DOI: 10.1039/d1cc05904a

rsc.li/chemcomm

# 2.2.2-Cryptand complexes of neptunium(III) and plutonium(III)†

Conrad A. P. Goodwin, (1) ‡ Sierra R. Ciccone, (1) ‡ Samuel Bekoe, (1) S Sourav Majumdar, Db Brian L. Scott, Dc Joseph W. Ziller, Db Andrew J. Gaunt. \*\* Filipp Furche\*\* and William J. Evans \*\*\*

New coordination environments are reported for Np(III) and Pu(III) based on pilot studies of U(III) in 2.2.2-cryptand (crypt). The U(III)-incrypt complex, [U(crypt)I2][I], obtained from the reaction between UI<sub>3</sub> and crypt, is treated with Me<sub>3</sub>SiOTf (OTf = O<sub>3</sub>SCF<sub>3</sub>) in benzene to form the [U(crypt)(OTf)2][OTf] complex. Similarly, the isomorphous Np(III) and Pu(III) complexes were obtained similarly starting from  $[Anl_3(THF)_4]$ . All three complexes (1-An; An = U, Np, Pu) contain an encapsulated actinide in a THF-soluble complex. Absorption spectroscopy and DFT calculations are consistent with 5f<sup>3</sup> U(III), 5f<sup>4</sup> Np(III), and 5f<sup>5</sup> Pu(III) electron configurations.

Expanding the coordination chemistry of the transuranium metals can achieve a better understanding of the chemistry of the actinide series. The limited availability of transuranium isotopes to basic research laboratories coupled with their radiological hazards limits the reaction scales and scientific breadth. In contrast, thorium and uranium chemistry is better developed than the rest of the actinide series. 1d,2,3 Described here is a reaction system, using the 2.2.2cryptand (crypt) ligand, 4,7,13,16,21,24-hexaoxa-1,10-diazabicyclo-

and two nitrogen donor atoms.4 It has been used extensively to encapsulate many types of metal ions, 4,5 but it is mostly known for its high affinity for potassium and other alkali and alkaline earth metals. Recently, crypt has been used with Ln(II) ions<sup>6</sup> (Ln = lanthanide), but the application of this ligand system to the coordination chemistry of the actinides has been less studied. 6h,7 Spectroscopic and elemental analytical data on U(IV) and U(VI) crypt complexes have been reported in the literature as early as 1976, 6h,7a,d-f but the first X-ray crystal structures of uranium crypt complexes were only recently reported in 2018 on the U(III) complexes  $[U(crypt)I_2][I]$ ,  $[U(crypt)(OH_2)][I]_2$ , and  $[U(crypt)I(OH_2)]$ [I][BPh4].7c Additional crystallographic data were subsequently reported on [U(crypt)(MeCN)I][I]<sub>2</sub> and [U(crypt)(OH<sub>2</sub>)<sub>2</sub>][I]<sub>3</sub>·2MeCN.<sup>7b</sup>

Although these iodide complexes established the structural details of U(III)-in-crypt, they were only soluble in DMF and MeCN, which limited the utility of this encapsulating ligand environment for developing further actinide reaction chemistry. The closest encapsulating ligands in the Np and Pu literature involved 18-crown-6 (crown).8 However, these typically featured high-valent actinyl AnO2n+ centers or counteranions such as [ClO<sub>4</sub>] that diminished the solubility necessary for more extensive investigation of reactivity.8b However, studies of Ln-in-crypt complexes revealed that triflate counteranions were useful in increasing the solubility of 4f element crypt compounds<sup>6g,7b</sup> In addition, triflates were used as ancillary ligands for an electrochemical study of the effect of crypt on redox potentials of in situ generated putative Cf complexes.6g

We describe the isolation of a THF-soluble U(III)-in-crypt triflate complex that can be generated and crystallized quickly on a small-scale, such that the synthesis is viable for analogous Np(III) and Pu(III) complexes. This has provided Np and Pu in the polydentate coordination environment of crypt for the first time. Previous attempts to synthesize a THF soluble U(III)-incrypt complex involved the reaction of a solution of KOTf with the THF-insoluble brown-green complex [U(crypt)I<sub>2</sub>][I].<sup>7c</sup> This generated a green solution that upon workup was found to be [U(crypt)(OTf)<sub>2</sub>][OTf], 1-U. While this method provided a route to yield single crystals of 1-U, it was difficult to isolate analytically pure material and the crystals grew slowly. Therefore, for

<sup>[8.8.8]</sup>hexacosane, that is readily extendable on small-scales from U(III) to Np(III) and Pu(III) to define new coordination environments for these transuranium elements. The crypt ligand is a polydentate bicyclic molecule with six oxygen

<sup>&</sup>lt;sup>a</sup> Chemistry Division, Los Alamos National Laboratory, Los Alamos, NM 87545, USA. E-mail: gaunt@lanl.gov

<sup>&</sup>lt;sup>b</sup> Department of Chemistry, University of California Irvine, Irvine, CA 92697-2025, USA. E-mail: wevans@uci.edu, filipp.furche@uci.edu

<sup>&</sup>lt;sup>c</sup> Materials Physics & Applications Division, Los Alamos National Laboratory, Los Alamos, NM 87545, USA

<sup>†</sup> Electronic supplementary information (ESI) available: Full experimental (including a hazard statement for handling transuranium isotopes) and calculation details, crystal data tables, and CIFs. CCDC 2109157-2109159. For ESI and crystallographic data in CIF or other electronic format see DOI: 10.1039/ d1cc05904a

<sup>‡</sup> These authors contributed equally to this work.

Communication ChemComm

Np and Pu an alternative synthesis using Me3SiOTf as the triflate ligand source was explored.

In an inert atmosphere argon glovebox, Me<sub>3</sub>SiOTf reacts with [U(crypt)I<sub>2</sub>][I] as a suspension in benzene to form a green oil that, upon workup and recrystallization from THF/Et2O, quickly gives pure single crystals of green 1-U, eqn (1), in 66% yield on a 100 mg scale. Various small-scale (11 mg) recrystallizations of crude 1-U were examined but the THF/Et2O combinations provided the best single crystals.

These small-scale optimizations were then successfully extended to Np and Pu using [AnI<sub>3</sub>(THF)<sub>4</sub>] starting materials.<sup>9</sup> In an inert atmosphere, negative pressure helium atmosphere glovebox, a 15 mg sample of orange-colored [NpI<sub>3</sub>(THF)<sub>4</sub>] reacts with crypt in THF to form a yellow suspension that is presumed to be the analog of [U(crypt)I<sub>2</sub>][I] in eqn (1). A suspension of this yellow material in benzene reacts with Me<sub>3</sub>SiOTf to form a yellow powder that dissolves in THF, eqn (2). Recrystallization from THF/Et2O produced pale blue plates of [Np(crypt)(OTf)<sub>2</sub>][OTf], **1-Np**, identified by X-ray crystallography, in 79% yield based on the [NpI<sub>3</sub>(THF)<sub>4</sub>] starting material, Fig. 1.

Similarly, 25 mg of the cream-colored [PuI<sub>3</sub>(THF)<sub>4</sub>] reacted with crypt in f to form a cream-colored precipitate that then

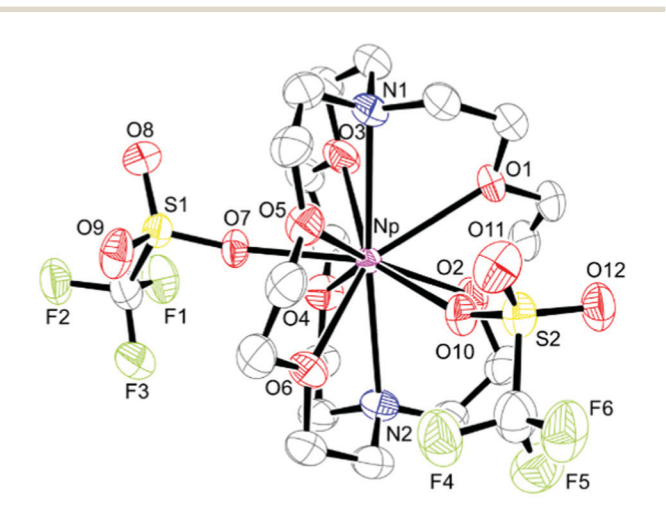


Fig. 1 Representation of 1-Np with atomic displacement parameters drawn at the 30% probability level. Hydrogen atoms are omitted for clarity, as is the non-coordinating triflate anion. 1-U is isomorphous.

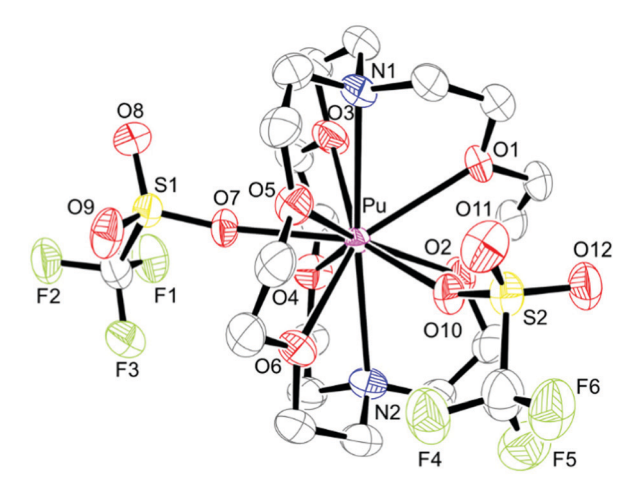


Fig. 2 Representation of 1-Pu with atomic displacement parameters drawn at the 30% probability level. Hydrogen atoms are omitted for clarity, as is the non-coordinating triflate anion.

reacts with Me<sub>3</sub>SiOTf in benzene to form [Pu(crypt)(OTf)<sub>2</sub>][OTf], 1-Pu, as pale lilac plates in 14% yield, Fig. 2, eqn (2). The lower vield for Pu is probably due to the difficulties in obtaining single crystals of 1-Pu of X-ray diffraction quality, which required multiple recrystallizations.

Structural data on 1-U, 1-Np, and 1-Pu are presented in Table 1. The complexes crystallize in the  $P\bar{1}$  space group and are isomorphous. Each structure contains an [An(crypt)(OTf)<sub>2</sub>]<sup>1+</sup> cation that approximates to a 10-coordinate tetra-capped trigonal prism with the nitrogen donors capping both trigonal faces and the triflate oxygens capping two of the rectangular faces. A third triflate anion is present and well separated from the [An(crypt)(OTf)<sub>2</sub>]<sup>1+</sup> cations. There are three formula units within the asymmetric unit that give a wide range of distances, for example, in 1-Pu the Pu-O(OTf) range is 2.439(9)-2.512(9) Å across six unique bond distances (see Table 1). These Pu-O distances to the triflate anions are shorter than the range of Pu-O(crypt) distances (2.565(12)-2.677(13) Å) to the neutral oxygen donor sites of the crypt. The range of Pu-N(crypt) distances in 1-Pu (2.731(14)-2.834(17) Å) is the largest of the **1-An** series, containing both the shortest and longest An-N bonds.

There is no clear evidence of the expected trend of bond shortening due to increased charge density from U<sup>3+</sup> to Np<sup>3+</sup> to Pu<sup>3+</sup>. This could simply be due to the magnitude of error values in our data associated with the individual metal-ligand distances to relatively light O and N atoms, along with the wide spread of values precluding useful comparison of average values (large standard deviation). Higher resolution data may have revealed a trend. Unfortunately, the paucity of single crystal X-ray structural data across homologous trivalent series,

Table 1 Selected bond distances [Å] in [An(crypt)(OTf)<sub>2</sub>][OTf], 1-An

	An-O(OTf)	An-O(crypt)	An-N(crypt)
1-U	2.454(4)-2.518(4)	2.566(4)-2.677(4)	2.754(5)-2.809(5)
1-Np	2.427(9)-2.512(9)	2.570(11)-2.659(13)	2.734(14)-2.775(17)
1-Pu	2.439(9)-2.512(9)	2.565(12)-2.677(13)	2.731(14)-2.834(17)

ChemComm Communication

extending from U-Pu, with neutral O-donor ligands provides limited contextualization of the 1-An data. However, the trivalent halide series [AnI<sub>3</sub>(THF)<sub>4</sub>] (An = U, Np, Pu), where there is just a single molecule per asymmetric unit, do show An-O(THF) bond length shortening from U to Np to Pu, though also exhibiting a wide range of values for each metal (e.g. An-O bond lengths for An = U, 2.502(5)-2.563(5) Å; Np, 2.481(5)-2.550(5) Å; Pu, 2.445(3)-2.521(4) Å) but with  $3\sigma$  overlap between the shortest U-O and Np-O distances. 11 The ninecoordinate tricapped trigonal prismatic  $[An(H_2O)_9]^{3+}$  structures have An-O(prismatic) distances that decrease more consistently than the An-O(capping) distances, but still with some An-O distances exhibiting overlap (between next-neighbor elements) at the  $3\sigma$  level of statistical significance. These comparisons highlight the difficultly in unambiguously observing decreasing An3+-ligand (An = U, Np, Pu) distances with relatively light atom donors.

The <sup>19</sup>F NMR resonances of 1-U (-79.93 ppm), 1-Np (-82.22 ppm), and **1-Pu** (-79.77 ppm) in THF- $d_8$  all show a single resonance which indicates that the triflate anions are equivalent in solution, presumably due to rapid exchange on the NMR timescale. They are only slightly shifted from that of KOTf at -79.54 ppm. Similarly, the <sup>1</sup>H NMR spectra of **1-Np** and 1-Pu each show just a single set of three resonances assigned to the crypt ligand: 1-Np, 10.85, 6.12, and 1.14 ppm; 1-Pu, 4.29, 4.05, and 3.23 ppm, indicating that in solution it is in a symmetric environment. This indicates that in solution there is  $C_3$  symmetry in contrast to the solid-state structures that contain two coordinated OTf anions. These <sup>1</sup>H NMR resonances are shifted slightly from the values for free crypt at 3.60, 3.52, and 2.57 ppm. These small shifts are consistent with other NMR spectra of Np(III) and Pu(III). 9,13 The room temperature <sup>1</sup>H NMR spectrum of 1-U in THF-d<sub>8</sub> has a single discernible broad signal at -8.25 ppm within a window of 300 ppm to -150 ppm. This differs from the  $^{1}$ H NMR spectrum of  $[U(crypt)I_2][I]$  in MeCN- $d_3$  which contains resonances at 8.39, 6.86 and 5.97 ppm. The broad resonance of 1-U splits into several broad resonances at 260 K, but a clearly resolved threeline spectrum was not obtained down to 245 K.

The experimental solution UV-vis-NIR spectra of the 1-An compounds are shown in Fig. 3 (black lines) alongside TDDFT

simulated spectra (see below). Each complex has numerous weak transitions at low energy in the f-f transition region (ca.  $7000-15\,000 \text{ cm}^{-1}$ ; 700-1400 nm) and large absorptions at energies over 20 000 cm<sup>-1</sup> (500 nm) that extend into the UV region which are plausibly charge transfer bands or  $5f \rightarrow 6d$ transitions. Electronic structure calculations on the [An(crypt)(OTf)<sub>2</sub>]<sup>1+</sup> complexes were carried out at the density functional level of theory using the TPSSh14 functional with Grimme's D3 dispersion correction<sup>15</sup> in  $C_1$  symmetry to evaluate the ground state nature of these complexes and their UVvisible spectra. All calculations were carried out with the TURBOMOLE program suite, Version V-7.5. 16 The calculations indicated quartet 5f3, quintet 5f4, and sextet 5f5 ground state configurations for [U(crypt)(OTf)<sub>2</sub>]<sup>1+</sup>, [Np(crypt)(OTf)<sub>2</sub>]<sup>1+</sup>, and [Pu(crypt)(OTf)<sub>2</sub>]<sup>1+</sup>, respectively. The calculated average An-O and An-N bond distances are within 0.02 Å of the experimental values in [An(crypt)(OTf)<sub>2</sub>][OTf].

TDDFT calculations of the simulated UV-vis-NIR spectra are shown in Fig. 3 (green lines). For all three complexes  $[U(crypt)(OTf)_2]^{1+}$ ,  $[Np(crypt)(OTf)_2]^{1+}$ , and  $[Pu(crypt)(OTf)_2]^{1+}$ , the calculations indicate that there are very weak  $5f \rightarrow 5f$ transitions in the 7000-20000 cm<sup>-1</sup> region and intense  $5f \rightarrow 6d$  transitions at energies over 20 000 cm<sup>-1</sup>. Although scalar relativistic DFT calculations do not provide accurate estimates of intensity and splitting patterns of these  $5f \rightarrow 5f$ transitions, the overall match of the UV-visible spectra in the  $5f \rightarrow 6d$  region and the absence of  $6d \rightarrow 7p$  transitions (characteristic of divalent actinide compounds with 6d<sup>1</sup> ground states)<sup>17</sup> supports the assignment of 5f<sup>n</sup> ground states with no 6d occupation. The onset of  $5f \rightarrow 6d$  transitions occurs at higher energies in the order U < Np < Pu, in keeping with the increasing stabilization of the 5f manifold relative to the 6d orbitals as the actinide series is traversed from U to Np to Pu. Since TDDFT excitation calculations are susceptible to spurious charge transfer excitations from weakly bound anions, the spectra were also modelled with triflate-free cations [An(crypt)]<sup>3+</sup>. However, the [An(crypt)(OTf)<sub>2</sub>]<sup>1+</sup> calculations provided the better match and are shown here. Calculations with [An(crypt)]<sup>3+</sup> are included in the ESI† for comparison.

In summary, the coordination chemistry of 2.2.2-cryptand has been expanded to Np(III) and Pu(III) through methods

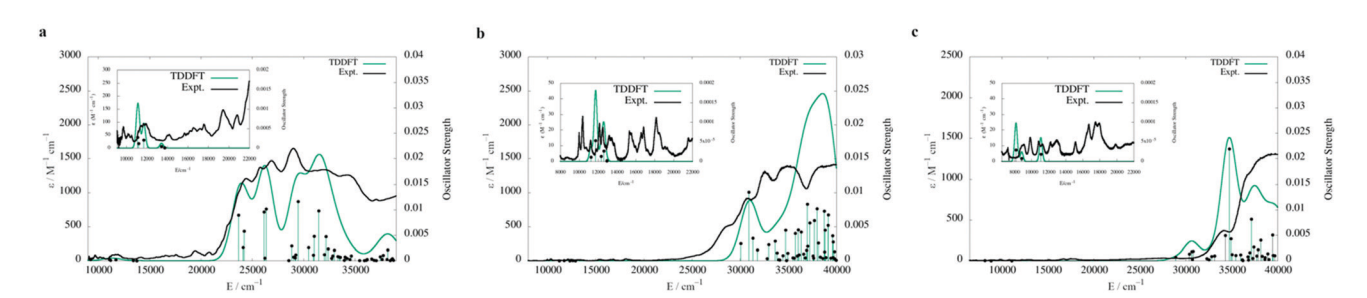


Fig. 3 Black lines show solution UV-vis-NIR spectra of (a) [U(crypt)(OTf)<sub>2</sub>][OTf] (1-U) (5 mM), (b) 1-Np (1.89 mM), and (c) 1-Pu (2.05 mM) in THF at ambient temperature. Green lines show simulated UV-vis-NIR spectra of (a)  $[U(crypt)(OTf)_2]^{1+}$ , (b)  $[Np(crypt)(OTf)_2]^{1+}$ , and (c)  $[Pu(crypt)(OTf)_2]^{1+}$  with computed TDDFT oscillator strengths shown as vertical lines. The experimental spectrum is shown in black for comparison. A Gaussian line broadening of 0.10 eV was applied. The computed intensities were scaled (see ESI† for details) to ease comparison with the experiment spectrum.

initially found to be successful for U(III). The U(III)-in-crypt complex, [U(crypt)I2][I], reacts with Me3SiOTf to generate [U(crypt)(OTf)<sub>2</sub>][OTf]. Using analogous procedures, crystallographically characterizable [An(crypt)(OTf)<sub>2</sub>][OTf] complexes of Np and Pu could be prepared and isolated. The transuranic complexes are isomorphous with the U analog and all are THFsoluble. The solubility provides the opportunity to use this encapsulating coordination environment for further development of transuranium chemistry. DFT calculations reveal 5f<sup>n</sup> ground-state electronic configurations in accord with that for trivalent ions. TDDFT performed [An(crypt)(OTf)<sub>2</sub>]<sup>1+</sup> show UV-vis-NIR features that agree well with the experimental spectra for all three metals. These combined theoretical/experimental results reveal a clear and simple physical manifestation of increased 5f-6d energetic separation across the series from U to Np to Pu.

We gratefully acknowledge the US. Department of Energy, Office of Science (DOE-OS), Basic Energy Sciences (BES) Heavy Element Chemistry (HEC) Program (W. J. E., S. R. C., J. W. Z.; award DE-SC0004739 and B. L. S.; award DE-AC52-06NA25396), the Los Alamos National Laboratory (LANL), Laboratory Directed Research and Development (LDRD) Exploratory Research Program (A. J. G.; award 20190091ER) and calculations were based upon work supported by the US National Science Foundation, Office of Advanced Cyberinfrastructure (S. B., S. M., F. F.; OAC-1835909). CAPG was sponsored by a Distinguished J. R. Oppenheimer Postdoctoral Fellowship (LANL-LDRD 20180703PRD1).

#### Conflicts of interest

Communication

Filipp Furche has an equity interest in TURBOMOLE GmbH. The terms of this arrangement have been reviewed and approved by the University of California, Irvine, in accordance with its conflict of interest policies.

#### Notes and references

- 1 (a) F. D. White and M. L. Marsh, Handbook on the Physics and Chemistry of Rare Earths, 2019, ch. Including Actinides, vol. 55, pp. 123-158; (b) P. L. Arnold, M. S. Dutkiewicz and O. Walter, Chem. Rev., 2017, 117, 11460-11475; (c) N. Kaltsoyannis, Chem. - Eur. J., 2018, 24, 2815-2825; (d) M. B. Jones and A. J. Gaunt, Chem. Rev., 2013, 113, 1137-1198.
- 2 (a) S. G. Minasian, J. L. Krinsky and J. Arnold, Chem. Eur. J., 2011, 17, 12234-12245; (b) S. E. Gilson and P. C. Burns, Coord. Chem. Rev., 2021, 445, 213994; (c) T. E. Albrecht-Schmitt, Organometallic and Coordination Chemistry of the Actinides, 2008; (d) A. R. Fox, S. C. Bart, K. Meyer and C. C. Cummins, Nature, 2008, 455, 341-349; (e) L. R. Morss, N. M. Edelstein and J. Fuger, The Chemistry of the Actinide and Transactinide Elements, 2011; (f) T. W. Hayton, Dalton Trans., 2010, 39, 1145-1158; (g) M. Ephritikhine, Dalton Trans., 2006, 2501-2516; (h) S. T. Liddle, Angew. Chem., Int. Ed., 2015, 54, 8604-8641.
- 3 C. R. Groom, I. J. Bruno, M. P. Lightfoot and S. C. Ward, Acta Crystallogr., Sect. B: Struct. Sci., Cryst. Eng. Mater., 2016, 72, 171-179.
- 4 (a) B. Dietrich, J. M. Lehn and J. P. Sauvage, Tetrahedron, 1973, 29, 1647–1658; (b) B. Dietrich, J. M. Lehn, J. P. Sauvage and J. Blanzat, Tetrahedron, 1973, 29, 1629-1645.
- 5 (a) J. M. Lehn, Pure Appl. Chem., 1977, 49, 857-870; (b) J. M. Lehn, Acc. Chem. Res., 2002, 11, 49-57.

- 6 (a) L. A. Ekanger, L. A. Polin, Y. Shen, E. M. Haacke, P. D. Martin and M. J. Allen, Angew. Chem., Int. Ed., 2015, 54, 14398-14401; (b) N. D. Gamage, Y. Mei, J. Garcia and M. J. Allen, Angew. Chem., Int. Ed., 2010, 49, 8923-8925; (c) D. N. Huh, S. R. Ciccone, S. Bekoe, S. Roy, J. W. Ziller, F. Furche and W. J. Evans, Angew. Chem., Int. Ed., 2020, **59**, 16141–16146; (d) D. N. Huh, C. M. Kotyk, M. Gembicky, A. L. Rheingold, J. W. Ziller and W. J. Evans, Chem. Commun., 2017, 53, 8664-8666; (e) T. C. Jenks, A. N. W. Kuda-Wedagedara, M. D. Bailey, C. L. Ward and M. J. Allen, Inorg. Chem., 2020, 59, 2613-2620; (f) C. U. Lenora, F. Carniato, Y. Shen, Z. Latif, E. M. Haacke, P. D. Martin, M. Botta and M. J. Allen, Chem. - Eur. J., 2017, 23, 15404-15414; (g) M. L. Marsh, F. D. White, D. S. Meeker, C. D. McKinley, D. Dan, C. Van Alstine, T. N. Poe, D. L. Gray, D. E. Hobart and T. E. Albrecht-Schmitt, Inorg. Chem., 2019, 58, 9602-9612; (h) T. N. Poe, M. J. Beltran-Leiva, C. Celis-Barros, W. L. Nelson, J. M. Sperling, R. E. Baumbach, H. Ramanantoanina, M. Speldrich and T. E. Albrecht-Schönzart,
- 7 (a) B. Spiess, F. Arnaud-Neu and M. J. Schwing-Weill, Inorg. Nucl. Chem. Lett., 1979, 15, 13-16; (b) D. N. Huh, J. M. Barlow, S. R. Ciccone, J. W. Ziller, J. Y. Yang and W. J. Evans, Inorg. Chem., 2020, **59**, 17077–17083; (c) D. N. Huh, C. J. Windorff, J. W. Ziller and W. J. Evans, Chem. Commun., 2018, 54, 10272-10275; (d) M. Brighli, P. Fux, J. Lagrange and P. Lagrange, Inorg. Chem., 2002, 24, 80-84; (e) R. M. Costes, G. Folcher, P. Plurien and P. Rigny, Inorg. Nucl. Chem. Lett., 1976, 12, 491-499; (f) J. I. Bullock and A. E. Storey, Inorg. Chim. Acta, 1979, 36, L399-L400.

Inorg. Chem., 2021, 60, 7815-7826.

- 8 (a) David L. Clark, D. Webster Keogh, Phillip D. Palmer, Brian L. Scott and C. D. Tait, Angew. Chem., Int. Ed., 1998, 37, 164-166; (b) K. Li, S. Hu, Q. Zou, Y. Zhang, H. Zhang, Y. Zhao, T. Zhou, Z. Chai and Y. Wang, Inorg. Chem., 2021, 60, 8984-8989; (c) M. M. Pyrch, J. M. Williams and T. Z. Forbes, Chem. Commun., 2019, 55, 9319-9322; (d) Y. Wang, S.-X. Hu, L. Cheng, C. Liang, X. Yin, H. Zhang, A. Li, D. Sheng, J. Diwu, X. Wang, J. Li, Z. Chai and S. Wang, CCS Chem., 2020, 2, 425-431.
- 9 C. A. P. Goodwin, M. T. Janicke, B. L. Scott and A. J. Gaunt, J. Am. Chem. Soc., 2021, 143, 20680-20696.
- 10 R. D. Shannon, Acta Crystallogr., Sect. A: Cryst. Phys., Diffr., Theor. Gen. Crystallogr., 1976, 32, 751-767.
- 11 (a) A. J. Gaunt, S. D. Reilly, A. E. Enriquez, T. W. Hayton, J. M. Boncella, B. L. Scott and M. P. Neu, Inorg. Chem., 2008, 47, 8412-8419; (b) F. W. Heinemann, S. Löffler and K. Meyer, 2018, CCDC 1876221: Experimental Crystal Structure Determination, Cambridge Crystallographic Data Centre.
- 12 C. Apostolidis, B. Schimmelpfennig, N. Magnani, P. Lindqvist-Reis, O. Walter, R. Sykora, A. Morgenstern, E. Colineau, R. Caciuffo, R. Klenze, R. G. Haire, J. Rebizant, F. Bruchertseifer and T. Fanghänel, Angew. Chem., Int. Ed., 2010, 49, 6343-6347.
- 13 (a) A. J. Myers, M. L. Tarlton, S. P. Kelley, W. W. Lukens and J. R. Walensky, Angew. Chem., Int. Ed., 2019, 58, 14891-14895; (b) J. Su, C. J. Windorff, E. R. Batista, W. J. Evans, A. J. Gaunt, M. T. Janicke, S. A. Kozimor, B. L. Scott, D. H. Woen and P. Yang, J. Am. Chem. Soc., 2018, 140, 7425-7428; (c) C. J. Windorff, G. P. Chen, J. N. Cross, W. J. Evans, F. Furche, A. J. Gaunt, M. T. Janicke, S. A. Kozimor and B. L. Scott, J. Am. Chem. Soc., 2017, 139, 3970-3973; (d) C. J. Windorff, J. M. Sperling, T. E. Albrecht-Schönzart, Z. Bai, W. J. Evans, A. N. Gaiser, A. J. Gaunt, C. A. P. Goodwin, D. E. Hobart, Z. K. Huffman, D. N. Huh, B. E. Klamm, T. N. Poe and E. Warzecha, Inorg. Chem., 2020, 59, 13301-13314.
- 14 V. N. Staroverov, G. E. Scuseria, J. Tao and J. P. Perdew, J. Chem. Phys., 2003, 119, 12129-12137.
- 15 (a) S. Grimme, J. Comput. Chem., 2006, 27, 1787-1799; (b) S. Grimme, J. Antony, S. Ehrlich and H. Krieg, J. Chem. Phys., 2010, 132, 154104,
- 16 TURBOMOLE V7.5 2020, a development of University of Karlsruhe and Forschungszentrum Karlsruhe GmbH, 1989-2007, TURBO-MOLE GmbH, since 2007; available from https://www.turbomole. org.
- 17 J. C. Wedal, S. Bekoe, J. W. Ziller, F. Furche and W. J. Evans, Organometallics, 2020, 39, 3425-3432.